

Addressing Positivity Violations in Causal Effect Estimation using Gaussian Process Priors

Yaqian Zhu, Nandita Mitra [♣], Jason Roy [♣]

[♣]Co-senior authors

Abstract

In observational studies, causal inference relies on several key identifying assumptions. One identifiability condition is the positivity assumption, which requires the probability of treatment be bounded away from 0 and 1. That is, for every covariate combination, it should be possible to observe both treated and control subjects, i.e., the covariate distributions should overlap between treatment arms. If the positivity assumption is violated, population-level causal inference necessarily involves some extrapolation. Ideally, a greater amount of uncertainty about the causal effect estimate should be reflected in such situations. With that goal in mind, we construct a Gaussian process model for estimating treatment effects in the presence of practical violations of positivity. Advantages of our method include minimal distributional assumptions, a cohesive model for estimating treatment effects, and more uncertainty associated with areas in the covariate space where there is less overlap. We assess the performance of our approach with respect to bias and efficiency using simulation studies. The method is then applied to a study of critically ill female patients to examine the effect of undergoing right heart catheterization.

1 Introduction

Researchers often aim to infer the causal effects of a treatment on a population of interest from observational studies. Identification of causal effects from observational data relies on assumptions including ignorability, often referred to as “no unmeasured confounding,” which holds when treatment assignment is random (that is, independent of potential outcomes) given measured confounders.¹ If the treatment received depends on observed covariates, then the distribution of these covariates is expected to differ by treatment group. This raises concerns about violations of a second identifying assumption called positivity. Positivity assumes that there is a non-zero probability of receiving treatment for all individuals. If there is a subpopulation defined by covariates for which one of the treatments is not observed, causal contrasts for that subgroup cannot be identified without further assumptions.^{2;3}

Theoretical (or structural) violation of the positivity assumption occurs when a subpopulation of individuals have zero probability of receiving at least one of the treatments, so that even if we let the sample size go to infinity, we would still never observe all treatment values. This can happen, for example, when treatment is contraindicated in a certain subgroup of patients because of their age, comorbidities, and family history of disease. D’Amour et al. (2020) elaborate on this type of violation in the context of high-dimensional covariates.⁴ On the other hand, practical (also called random) violation of positivity arises when, in a given observational data set, a subpopulation is not observed to receive a particular treatment by chance. For example, suppose in a sample, no males between the ages of 35 to 45 receive treatment A purely by chance. In reality, their probability of receiving treatment A may be small but not zero. In this case, we will not be able to learn about the treatment effect of A in this subpopulation of men without making additional modeling assumptions. We expect practical positivity violations to arise in clinical data, especially when there are a large number of covariates. However, we could potentially learn about these nonoverlap regions using modeling. For instance, if we are willing to assume an additive linear regression model, we could learn about males treated with treatment A via linear interpolation or extrapolation from younger or older men who received treatment A . The disadvantage is that we would need to

rely on strong parametric assumptions.⁵ Further, these approaches may underestimate the degree of uncertainty that would be expected in data-sparse regions.

Trimming approaches are commonly used to address positivity violations and are discussed in Petersen et al. (2012).⁶ Crump et al. (2009) propose a method that removes (trims) subjects whose propensity scores are outside specified bounds and calculates a minimum variance estimate on the remaining subsample.⁷ This approach requires correct specification of the propensity score model and may result in a final sample that is a small subsample of the original study population. Others (Rosenbaum (2012) and Visconti & Zubizarreta (2018)) have suggested matching treated and control subjects on covariates or propensity scores;^{8;9} however, external validity may be diminished due to matching because the target population of interest will have changed to that of the matched population. Hill & Su (2013) define nonoverlap as the set of subjects whose estimated individual causal effects have corresponding variances that are greater than specified upper bounds.¹⁰ However, these upper bound cut-offs may rely on user specifications and may not adequately reflect the amount of data sparsity. Ghosh (2018) characterizes multivariate covariate overlap using convex hulls to determine positivity violations.¹¹ This overlap subset is termed ‘the margin’ and is determined using a propensity score model; subjects who are outside the margin are trimmed. A disadvantage to these trimming procedures is that by discarding subjects, the target of inference may shift to a resulting subpopulation which may not represent the original population of interest.

An alternative to removing subjects entirely is to downweight subjects in regions with less overlap. In that spirit, Li et al. (2018) proposed estimating causal effects using overlap weights.^{12;13} However, overlap weights involve propensity score estimation and place more emphasis on those with higher probabilities of receiving either treatment.

Although trimming or weighting approaches may be appropriate for structural violations, they fall short for practical violations of the positivity assumption. When there are practical but not structural violations, interest generally centers on understanding the treatment effects for the entire population. Approaches that account for positivity violations while also targeting a causal estimand for the whole population are, therefore, of most interest.

There has been some recent work on methods that are based on extrapolating information from overlap regions to nonoverlap regions in a way that preserves the intended target of inference. For instance, Nethery et al. (2019) propose a method for estimating a causal effect on the entire population using extrapolation.¹⁴ Their definition of the overlap region relies on two user-specified parameters that indicate the desired extent of closeness between treatment groups based on subjects’ estimated propensity scores. Choices regarding propensity score model specification and user inputs influence whether a subject is included in the overlap region. Having a fixed region means that uncertainty around subjects’ inclusion in the overlap or nonoverlap region is ignored. In this approach, treatment stratified Bayesian additive regression tree (BART) models are used to estimate causal effects for the overlap regions and then in a subsequent stage, spline (SPL) models extrapolate those trends to subjects in the nonoverlap region. Because treated and control subjects are modeled separately, prior information on the treatment effect cannot be directly utilized. Lastly, although they account for the greater uncertainty in areas of nonoverlap, their proposed variance inflation strategy results in over-coverage as seen in their simulation studies.

To address some of the above limitations of existing approaches, we propose a Gaussian process modeling approach for estimating average treatment effects in a way that preserves the original target of inference.^{15;16} Our method contributes several advances to the current literature. First, because we use a non-parametric prior distribution, we avoid making parametric modeling assumptions. Further, the prior does not rely on user-specified parameters nor cut-offs to define regions of overlap. The amount of nonoverlap is accounted for in the covariance functions of the Gaussian process as the distances of a subject’s covariate values from those of individuals in the other treatment group. This avoids the need to construct explicit overlap and nonoverlap groups. Also, the further subjects are from each other in terms of their covariate values, the larger the variances, which reflects the underlying point that there should be greater uncertainty around estimated causal effects when there is less overlap.

The remainder of the article is organized as follows. In section 2, we formulate the Gaussian process model and present the Bayesian inferential framework with its priors, likelihood, and posteriors. In Section 3, we conduct simulation studies to assess the performance of our method compared to other current approaches. We then apply our approach to data from an observational study of right heart catheterization in female patients in Section 4. Section 5 provides a discussion of results and offers concluding remarks.

2 The Gaussian Process Model and Posterior Computation

2.1 Notation and Framework for Causal Effect Estimation

Here, we use the potential outcomes framework for estimating causal effects.¹⁷ Suppose there are n i.i.d. observations from a population. For each subject i in the sample, let A_i be the treatment assignment indicator with $A_i = 1$ if subject i receives the treatment of interest and $A_i = 0$ if subject i receives the control. For a dichotomous treatment, each subject i has two potential outcomes: $Y_i(1)$, the outcome under treatment, and $Y_i(0)$, the outcome under control. However, each subject may only receive one treatment in a study; that is, the observed outcome for subject i is $Y_i = A_i Y_i(1) + (1 - A_i) Y_i(0)$. Furthermore, define \mathbf{X}_i to be a vector of p pre-treatment variables or covariates.

Our target parameter of interest is the mean difference in potential outcomes under treatment and under control, respectively, given by $\Psi = E[Y(1) - Y(0)]$. This represents the average effect had everyone been given treatment versus had everyone been given control. Identifiability of this parameter rests on the following assumptions.^{18;19}

1. Consistency: $Y = Y(a)$ whenever $A = a$.
2. Stable Unit Treatment Value Assumption (SUTVA): there is only one form of treatment and one form of control, and there is no between-subject interference.
3. Ignorability: Conditional on covariates, treatment assignment is independent of the set of potential outcomes, $A \perp\!\!\!\perp \{Y(0), Y(1)\} | X$. This essentially says that there can be no unmeasured confounding.
4. Positivity: The probability of receiving either treatment given the covariates is nonzero, $0 < P(A = 1 | X) < 1$.

2.2 Gaussian Process Model

We assume the model for the continuous outcome Y given confounders X and treatment A has the following form,²⁰

$$Y_i = \mu(X_i) + \Delta(X_i)A_i + \epsilon_i, \text{ where } \epsilon_i \sim N(0, \sigma^2).$$

The function $\mu(X_i)$ represents the relationship between X and Y that is not part of the treatment effect; that is, it is the prognostic impact of covariates. The function $\Delta(X_i)$, which is a functional coefficient of A_i , can be thought of as representing conditional treatment effects, reflecting interactions between covariates and treatment. Under the causal assumptions described above, the average causal effect is just $\Psi = E(\Delta(X))$.

We treat the functional form of $\mu()$ and $\Delta()$ as unknown, and therefore need to specify priors for those functions. We assume independent Gaussian process priors for these functions. Specifically,

$$\begin{aligned} \mu(X) &\sim GP(X\beta, \mathcal{K}_\mu), \\ \Delta(X) &\sim GP(0, \mathcal{K}_\Delta). \end{aligned}$$

The mean function in the prior for $\mu(X)$ centers this parameter on a linear model, $X\beta$, while the mean function for $\Delta(X)$ is zero to reflect the a priori belief of small heterogeneous treatment effects. An advantage of GP priors is that we can center the priors on a parametric model. Essentially, the prior mean based on these functions is a linear model with no effect modification. Thus, when there is limited data, the outcome model will shrink towards this prior specification.

With the goal of having a noisier mean function when there is less overlap, we choose the squared exponential form for the covariance functions. For matrices of covariate values $X = \{\mathbf{X}_1, \dots, \mathbf{X}_p\}$ and $X^* = \{\mathbf{X}_1^*, \dots, \mathbf{X}_p^*\}$, the covariance function \mathcal{K}_Δ is defined to be

$$\mathcal{K}_\Delta(X, X^* | l_\Delta, \eta_\Delta) = \eta_\Delta^2 \exp \left\{ -\frac{1}{2} \left[\frac{|X - X^*|}{l_\Delta} \right]^2 \right\}.$$

The (i, j) th element of the covariance matrix \mathcal{K}_Δ would be

$$K_{\Delta,ij} = \mathcal{K}_\Delta(X(i), X^*(j)) = \eta_\Delta^2 \exp \left\{ -\frac{1}{2} \sum_{p=1}^P \left[\frac{X_p(i) - X_p^*(j)}{l_\Delta} \right]^2 \right\}.$$

$X_p(i)$ is the value of the p th covariate value for subject i , and $X_p^*(j)$ is the p th covariate value for subject j , $p = 1, \dots, P$. The covariance \mathcal{K}_μ has the same form, but with different parameters, l_μ and η_μ . The reason that this particular covariance function is useful when there are practical violations of the positivity assumption is that the variability of the function increases as distance between covariates increases, which we later show using the posterior distribution of Δ .

The parameters l_μ and l_Δ are the length scales which characterize the extent to which μ and Δ values change as the input changes.¹⁶ Small values correspond to more frequent changes in the parameter values for the same change in inputs X ; that is, the distance in X needed for the parameters to vary by an amount comparable to its range is smaller for small length scales. Increasing this hyperparameter reduces the amount of fluctuation. The parameters η_μ and η_Δ are the signal variances (output-scale amplitude). For η near 0, posterior mean estimates of the parameters tend to be more smooth with fewer fluctuations in the curve (closer to a straight line). At larger η values, regions with nonoverlap will have more variability associated with the corresponding conditional causal effect.

2.3 Priors, Likelihood, and Posteriors

The outcome given treatment and confounders is distributed as $Y \sim MVN(\mu + \Delta A, \sigma^2 I)$, which implies that the likelihood is

$$p(y|\mu, \Delta, \sigma^2) \propto \det(\sigma^2 I)^{-\frac{1}{2}} \exp \left[-\frac{1}{2} (y - (\mu + \Delta A))^T (\sigma^2 I)^{-1} (y - (\mu + \Delta A)) \right].$$

Note that $\mu = \mu(X)$ and $\Delta = \Delta(X)$ for simplification of notation. Also, $\Delta A = \begin{bmatrix} \Delta_1 A_1 \\ \vdots \\ \Delta_n A_n \end{bmatrix}$.

We specify priors for the hyperparameters

$$\begin{aligned} p(\beta) &\propto MVN(0, \sigma_\beta^2 I_P), \\ p(l_\mu) &\propto \text{gamma}(l_\mu | \alpha_{l_\mu}, \beta_{l_\mu}), \\ p(\eta_\mu) &\propto \text{gamma}(\eta_\mu | \alpha_{\eta_\mu}, \beta_{\eta_\mu}), \\ p(l_\Delta) &\propto \text{gamma}(l_\Delta | \alpha_{l_\Delta}, \beta_{l_\Delta}), \\ p(\eta_\Delta) &\propto \text{gamma}(\eta_\Delta | \alpha_{\eta_\Delta}, \beta_{\eta_\Delta}), \\ p(\sigma^2) &\propto \text{Inv-gamma}(\sigma^2 | \alpha_{\sigma^2}, \beta_{\sigma^2}). \end{aligned}$$

The vector of coefficients β is given a multivariate normal prior. This conjugate prior leads to a conditional posterior distribution for β that is also multivariate normal. The hyperparameters l and η are given gamma priors since their values need to be positive. The hyperparameter σ^2 has an inverse-gamma prior, which is a common prior for variance parameters. The joint prior is

$$p(\mu, \beta, l_\mu, \eta_\mu, \Delta, l_\Delta, \eta_\Delta, \sigma^2) \propto p(\mu|\beta, l_\mu, \eta_\mu) p(l_\mu) p(\beta) p(\eta_\mu) p(\Delta|l_\Delta, \eta_\Delta) p(l_\Delta) p(\eta_\Delta) p(\sigma^2),$$

which assumes a priori independence of the hyperparameters.

Then the joint posterior is

$$p(\mu, \beta, l_\mu, \eta_\mu, \Delta, l_\Delta, \eta_\Delta, \sigma^2 | Y) \propto p(y|\mu, \Delta, \sigma^2) p(\mu|\beta, l_\mu, \eta_\mu) p(\beta) p(l_\mu) p(\eta_\mu) p(\Delta|l_\Delta, \eta_\Delta) p(l_\Delta) p(\eta_\Delta) p(\sigma^2).$$

2.3.1 Conditional Posteriors

To ensure the Gaussian process priors for μ and Δ are not in too much disagreement with the data, we estimate hyperparameter values based on data and the posterior. That is, rather than choosing fixed values for the hyperparameters, l and η , in the GP priors, we assign them gamma priors as specified in the previous subsection and use Metropolis-Hastings to update their values. These are integrated in a Metropolis within Gibbs algorithm to obtain posterior inference for μ and Δ .²¹ The conditional distributions for β , μ , and Δ have analytical forms,

so estimates of these parameters may be drawn directly in their corresponding Gibbs steps.^{22;23} Because these conditional distributions are needed in the algorithm and are specific to the form of our Gaussian process model, we present them here. Detailed derivations are in Appendix A.

Since the choice of prior is $p(\beta) \propto \det(\sigma_\beta I_P)^{-1/2} \exp\left[-\frac{1}{2}\beta^T(\sigma_\beta^2 I_P)^{-1}\beta\right]$, the conditional posterior distribution for β is

$$\begin{aligned} p(\beta|\mu, y) &\propto p(y|\mu, \beta)p(\mu|\beta)p(\beta) \\ &\propto \exp\left[-\frac{1}{2}\{y - (\mu + \Delta A)\}^T (\sigma^2 I)^{-1} \{y - (\mu + \Delta A)\}\right] \exp\left[-\frac{1}{2}(\mu - X\beta)^T K_\mu^{-1}(\mu - X\beta)\right] \exp\left[-\frac{1}{2}\beta^T(\sigma_\beta^2 I_P)^{-1}\beta\right] \\ &\propto \exp\left(-\frac{1}{2}\left[\beta - \left\{X^T K_\mu^{-1} X + (\sigma_\beta^2 I_P)^{-1}\right\}^{-1} X^T K_\mu^{-1} \mu\right]^T \left\{X^T K_\mu^{-1} X + (\sigma_\beta^2 I_P)^{-1}\right\} \right. \\ &\quad \left. \left[\beta - \left\{X^T K_\mu^{-1} X + (\sigma_\beta^2 I_P)^{-1}\right\}^{-1} X^T K_\mu^{-1} \mu\right]\right) \end{aligned}$$

Thus, $\beta|\mu, y \sim MVN\left(\left[X^T K_\mu^{-1} X + (\sigma_\beta^2 I_P)^{-1}\right]^{-1} X^T K_\mu^{-1} \mu, \left[X^T K_\mu^{-1} X + (\sigma_\beta^2 I_P)^{-1}\right]^{-1}\right)$.

The posterior for $\mu|y$ is given by

$$\begin{aligned} p(\mu|\Delta, y) &\propto p(y|\mu, \Delta)p(\mu) \\ &\propto \det(\sigma^2 I)^{-\frac{1}{2}} \exp\left[-\frac{1}{2}\{y - (\mu + \Delta A)\}^T (\sigma^2 I)^{-1} \{y - (\mu + \Delta A)\}\right] \det(K_\mu)^{-\frac{1}{2}} \exp\left[-\frac{1}{2}(\mu - X\beta)^T K_\mu^{-1}(\mu - X\beta)\right] \\ &\propto \exp\left(-\frac{1}{2}\left[\mu - \left\{K_\mu^{-1} + (\sigma^2 I)^{-1}\right\}^{-1} \left\{(\sigma^2 I)^{-1}(y - \Delta A) + K_\mu^{-1} X\beta\right\}\right]^T \left\{K_\mu^{-1} + (\sigma^2 I)^{-1}\right\} \right. \\ &\quad \left. \left[\mu - \left\{K_\mu^{-1} + (\sigma^2 I)^{-1}\right\}^{-1} \left\{(\sigma^2 I)^{-1}(y - \Delta A) + K_\mu^{-1} X\beta\right\}\right]\right) \end{aligned}$$

Thus, $\mu|\beta, \Delta, y \sim MVN\left(\left[K_\mu^{-1} + (\sigma^2 I)^{-1}\right]^{-1} \left[(\sigma^2 I)^{-1}(y - \Delta A) + K_\mu^{-1} X\beta\right], \left[K_\mu^{-1} + (\sigma^2 I)^{-1}\right]^{-1}\right)$.

To obtain the conditional posterior for Δ , we first define some notation. Recall, A is the vector of treatment indicators for all the subjects, and let M denote a square matrix. $A^T \odot M$ indicates A is multiplied element-wise to each column of M while $M \odot A$ indicates A is multiplied element-wise to each row of M .

The posterior for $\Delta|\mu, y$ is given by

$$\begin{aligned} p(\Delta|\mu, y) &\propto p(y|\Delta, \mu)p(\Delta) \\ &\propto \det(\sigma^2 I)^{-\frac{1}{2}} \exp\left[(y - (\mu + \Delta A))^T (\sigma^2 I)^{-1} (y - (\mu + \Delta A))\right] \det(K_\Delta)^{-\frac{1}{2}} \exp\left(-\frac{1}{2}\Delta^T K_\Delta^{-1} \Delta\right) \\ &\propto \exp\left[-\frac{1}{2}\left(\Delta - [K_\Delta^{-1} + A^T \odot (\sigma^2 I)^{-1} \odot A]^{-1} A^T \odot (\sigma^2 I)^{-1} (y - \mu)\right)^T [K_\Delta^{-1} + A^T \odot (\sigma^2 I)^{-1} \odot A] \right. \\ &\quad \left. \left(\Delta - [K_\Delta^{-1} + A^T \odot (\sigma^2 I)^{-1} \odot A]^{-1} A^T \odot (\sigma^2 I)^{-1} (y - \mu)\right)\right] \end{aligned}$$

Thus, $\Delta|\mu, y \sim MVN\left(\left[K_\Delta^{-1} + A^T \odot (\sigma^2 I)^{-1} \odot A\right]^{-1} A^T \odot (\sigma^2 I)^{-1} (y - \mu), \left[K_\Delta^{-1} + A^T \odot (\sigma^2 I)^{-1} \odot A\right]^{-1}\right)$.

The posterior distribution for the treatment effects of all subjects has covariance matrix $[K_\Delta^{-1} + A^T \odot (\sigma^2 I)^{-1} \odot A]^{-1}$. Because it is difficult to write out the inverses, we obtain each element for the simple case with two subjects and a single covariate X . Let $A_1 = 1$ and X_1 denote the treatment status

and covariate for subject 1 and $A_2 = 0$ and X_2 denote the treatment status and covariate for subject 2, so that there is a treated subject and a control subject. The covariance matrix is given by

$$\left[K_{\Delta}^{-1} + A^T \odot (\sigma^2 I)^{-1} \odot A \right]^{-1} = \begin{bmatrix} \frac{\sigma^2 \eta_{\Delta}^2}{\sigma^2 + \eta_{\Delta}^2} & \frac{\sigma^2 \eta_{\Delta}^2}{\sigma^2 + \eta_{\Delta}^2} \exp \left\{ -\frac{1}{2} \left(\frac{X_1 - X_2}{l_{\Delta}} \right)^2 \right\} \\ \frac{\sigma^2 \eta_{\Delta}^2}{\sigma^2 + \eta_{\Delta}^2} \exp \left\{ -\frac{1}{2} \left(\frac{X_1 - X_2}{l_{\Delta}} \right)^2 \right\} & \eta_{\Delta}^2 \left[1 - \frac{\eta_{\Delta}^2}{\sigma^2 + \eta_{\Delta}^2} \exp \left\{ -\left(\frac{X_1 - X_2}{l_{\Delta}} \right)^2 \right\} \right] \end{bmatrix}$$

Subject 2's variance increases the further X_2 is from X_1 since a smaller amount would be subtracted from the second component of the product of $[K_{\Delta}^{-1} + A^T \odot (\sigma^2 I)]_{22}^{-1}$; that is, $\left[1 - \frac{\eta_{\Delta}^2}{\sigma^2 + \eta_{\Delta}^2} \exp \left\{ -\left(\frac{X_1 - X_2}{l_{\Delta}} \right)^2 \right\} \right]$ becomes larger when $|X_1 - X_2|$ increases. Thus, there is greater variability in the treatment effect posterior as $|X_1 - X_2|$ increases. This illustrates why with this prior specification we expect regions with little to no overlap to result in more uncertainty when it comes to causal effect estimation.

2.3.2 Metropolis within Gibbs Algorithm for Posterior Inference

In this section, we present the steps of the algorithm for obtaining posterior sampling of the parameters and hyperparameters. For the hyperparameters in the GP priors ($l_{\mu}, \eta_{\mu}, l_{\Delta}$, and η_{Δ}) and σ^2 , we use a Metropolis-Hastings step at each iteration and update their values based on current values of the other parameters using an acceptance ratio. For β, μ , and Δ , at each iteration, their new values are drawn from their respective conditional distributions given current values of all the other parameters. Let $l(\mu, \beta, l_{\mu}, \eta_{\mu}, \Delta, l_{\Delta}, \eta_{\Delta}, \sigma^2) = \log p(\mu, \beta, l_{\mu}, \eta_{\mu}, \Delta, l_{\Delta}, \eta_{\Delta}, \sigma^2 | Y)$ denote the log posterior distribution, and let $q(\cdot; m, s^2)$ be the density of the proposal distribution with mean m and variance s^2 . We start the chains with initial values

$$\mu^{(0)}, \beta^{(0)}, l_{\mu}^{(0)}, \eta_{\mu}^{(0)}, \Delta^{(0)}, l_{\Delta}^{(0)}, \eta_{\Delta}^{(0)}, \sigma^{2(0)}$$

At iteration j ,

1. Draw l_{μ}^* from the proposal distribution—truncated normal distribution centered at $l_{\mu}^{(j-1)}$ with variance $\tau_{l_{\mu}}^2$ and bounded below at 0:

$$l_{\mu}^* \sim TN(l_{\mu}^{(j-1)}, \tau_{l_{\mu}}^2; \text{lower} = 0)$$

$$\begin{aligned} \log r_{l_{\mu}} &= l(l_{\mu}^*, \eta_{\mu}^{(j-1)}, \beta^{(j-1)}, \mu^{(j-1)}, l_{\Delta}^{(j-1)}, \eta_{\Delta}^{(j-1)}, \Delta^{(j-1)}, \sigma^{2(j-1)}) \\ &\quad - l(l_{\mu}^{(j-1)}, \eta_{\mu}^{(j-1)}, \beta^{(j-1)}, \mu^{(j-1)}, l_{\Delta}^{(j-1)}, \eta_{\Delta}^{(j-1)}, \Delta^{(j-1)}, \sigma^{2(j-1)}) \\ &\quad + \log[q(l_{\mu}^{(j-1)}; l_{\mu}^*, \tau_{l_{\mu}}^2)] - \log[q(l_{\mu}^*; l_{\mu}^{(j-1)}, \tau_{l_{\mu}}^2)] \end{aligned}$$

We then draw a random $U \sim Unif(0, 1)$ and set

$$l_{\mu}^{(j)} = \begin{cases} l_{\mu}^*, & \text{if } \log U \leq \log r_{l_{\mu}} \\ l_{\mu}^{(j-1)}, & \text{otherwise} \end{cases}$$

2. Draw η_μ^* from the proposal distribution—truncated normal distribution centered at $\eta_\mu^{(j-1)}$ with variance $\tau_{\eta_\mu}^2$ and bounded below at 0:

$$\eta_\mu^* \sim TN(\eta_\mu^{(j-1)}, \tau_{\eta_\mu}^2; \text{lower} = 0)$$

$$\begin{aligned} \log r_{\eta_\mu} &= l(l_\mu^{(j)}, \eta_\mu^*, \beta^{(j-1)}, \mu^{(j-1)}, l_\Delta^{(j-1)}, \eta_\Delta^{(j-1)}, \Delta^{(j-1)}, \sigma^{2(j-1)}) \\ &\quad - l(l_\mu^{(j)}, \eta_\mu^{(j-1)}, \beta^{(j-1)}, \mu^{(j-1)}, l_\Delta^{(j-1)}, \eta_\Delta^{(j-1)}, \Delta^{(j-1)}, \sigma^{2(j-1)}) \\ &\quad + \log[q(\eta_\mu^{(j-1)}; \eta_\mu^*, \tau_{\eta_\mu}^2)] - \log[q(\eta_\mu^*; \eta_\mu^{(j-1)}, \tau_{\eta_\mu}^2)] \end{aligned}$$

We then draw a random $U \sim Unif(0, 1)$ and set

$$\eta_\mu^{(j)} = \begin{cases} \eta_\mu^*, & \text{if } \log U \leq \log r_{\eta_\mu} \\ \eta_\mu^{(j-1)}, & \text{otherwise} \end{cases}$$

3. Draw $\beta^{(j)}$ from

$$\begin{aligned} &MVN \left((X^T K_\mu(l_\mu^{(j)}, \eta_\mu^{(j)})^{-1} X + (\sigma_\beta^2 I_P)^{-1})^{-1} X^T K_\mu(l_\mu^{(j)}, \eta_\mu^{(j)})^{-1} \mu^{(j-1)}, \right. \\ &\quad \left. [X^T K_\mu(l_\mu^{(j)}, \eta_\mu^{(j)})^{-1} X + (\sigma_\beta^2 I_P)^{-1}]^{-1} \right) \end{aligned}$$

4. Draw $\mu^{(j)}$ from

$$\begin{aligned} &MVN([K_\mu(l_\mu^{(j)}, \eta_\mu^{(j)})^{-1} + (\sigma^{2(j-1)} I)^{-1}]^{-1} [(\sigma^{2(j-1)} I)^{-1} (y - \Delta^{(j-1)} A) + K_\mu^{-1} X \beta^{(j)}], \\ &\quad [K_\mu(l_\mu^{(j)}, \eta_\mu^{(j)})^{-1} + (\sigma^{2(j-1)} I)^{-1}]^{-1}) \end{aligned}$$

5. Draw l_Δ^* from its proposal distribution:

$$l_\Delta^* \sim TN(l_\Delta^{(j-1)}, \tau_{l_\Delta}^2; \text{lower} = 0)$$

$$\begin{aligned} \log r_{l_\Delta} &= l(l_\mu^{(j)}, \eta_\mu^{(j)}, \beta^{(j)}, \mu^{(j)}, l_\Delta^*, \eta_\Delta^{(j-1)}, \Delta^{(j-1)}, \sigma^{2(j-1)}) \\ &\quad - l(l_\mu^{(j)}, \eta_\mu^{(j)}, \beta^{(j)}, \mu^{(j)}, l_\Delta^{(j-1)}, \eta_\Delta^{(j-1)}, \Delta^{(j-1)}, \sigma^{2(j-1)}) \\ &\quad + \log[q(l_\Delta^{(j-1)}; l_\Delta^*, \tau_{l_\Delta}^2)] - \log[q(l_\Delta^*; l_\Delta^{(j-1)}, \tau_{l_\Delta}^2)] \end{aligned}$$

We then draw a random $U \sim Unif(0, 1)$ and set

$$l_\Delta^{(j)} = \begin{cases} l_\Delta^*, & \text{if } \log U \leq \log r_{l_\Delta} \\ l_\Delta^{(j-1)}, & \text{otherwise} \end{cases}$$

6. Draw η_Δ^* from its proposal distribution:

$$\eta_\Delta^* \sim TN(\eta_\Delta^{(j-1)}, \tau_{\eta_\Delta}^2; \text{lower} = 0)$$

$$\begin{aligned}
\log r_{\eta_\Delta} &= l(l_\mu^{(j)}, \eta_\mu^{(j)}, \beta^{(j)}, \mu^{(j)}, l_\Delta^{(j)}, \eta_\Delta^*, \Delta^{(j-1)}, \sigma^{2(j-1)}) \\
&\quad - l(l_\mu^{(j)}, \eta_\mu^{(j)}, \beta^{(j)}, \mu^{(j)}, l_\Delta^{(j)}, \eta_\Delta^{(j-1)}, \Delta^{(j-1)}, \sigma^{2(j-1)}) \\
&\quad + \log[q(\eta_\Delta^{(j-1)}; \eta_\Delta^*, \tau_{\eta_\Delta}^2)] - \log[q(\eta_\Delta^*; \eta_\Delta^{(j-1)}, \tau_{\eta_\Delta}^2)]
\end{aligned}$$

We then draw a random $U \sim Unif(0, 1)$ and set

$$\eta_\Delta^{(j)} = \begin{cases} \eta_\Delta^*, & \text{if } \log U \leq \log r_{\eta_\Delta} \\ \eta_\Delta^{(j-1)}, & \text{otherwise} \end{cases}$$

7. Draw $\Delta^{(j)}$ from

$$MVN([K_\Delta^{-1} + A^T \odot (\sigma^2 I)^{-1} \odot A]^{-1} A^T \odot (\sigma^2 I)^{-1} (y - \mu), [K_\Delta^{-1} + A^T \odot (\sigma^2 I)^{-1} \odot A]^{-1})$$

8. Draw σ^{2*} from its proposal distribution:

$$\sigma^{2*} \sim TN(\sigma^{2(j-1)}, \tau_{\sigma^2}^2; \text{lower} = 0)$$

$$\begin{aligned}
\log r_{\sigma^2} &= l(l_\mu^{(j)}, \eta_\mu^{(j)}, \beta^{(j)}, \mu^{(j)}, l_\Delta^{(j)}, \eta_\Delta^{(j)}, \Delta^{(j)}, \sigma^{2*}) \\
&\quad - l(l_\mu^{(j)}, \eta_\mu^{(j)}, \beta^{(j)}, \mu^{(j)}, l_\Delta^{(j)}, \eta_\Delta^{(j)}, \Delta^{(j)}, \sigma^{2(j-1)}) \\
&\quad + \log[q(\sigma^{2(j-1)}; \sigma^{2*}, \tau_{\sigma^2}^2)] - \log[q(\sigma^{2*}; \sigma^{2(j-1)}, \tau_{\sigma^2}^2)]
\end{aligned}$$

We then draw a random $U \sim Unif(0, 1)$ and set

$$\sigma^{2(j)} = \begin{cases} \sigma^{2*}, & \text{if } \log U \leq \log r_{\sigma^2} \\ \sigma^{2(j-1)}, & \text{otherwise} \end{cases}$$

This continues until the number the posterior draws after thinning and burn-ins (say, J) is reached. The effect estimate at iteration j is obtained as the mean over the elements of the $\Delta^{(j)}$ vector (i.e., the average across all subjects): $\psi^{(j)} = \frac{1}{n} \sum_{i=1}^n \Delta_i^{(j)}$. The average treatment effect is then estimated as the mean of the posterior draws of ψ , $\Psi = \frac{1}{J} \sum_{j=1}^J \psi^{(j)}$, so that estimation for continuous outcomes may be obtained directly from the posterior distribution of Δ .

2.4 Extension to Binary Outcomes

In this section, we extend our model to dichotomous outcomes where Y may take on the values of either 0 or 1. Let $\theta = \{\mu, \beta, l_\mu, \eta_\mu, \Delta, l_\Delta, \eta_\Delta\}$. The probit model assigns to each X_i the variable $Y_i \in \{0, 1\}$ using $P(Y_i = 1) = \Phi(f(X_i, A_i, \theta)) = \Phi(\mu(X_i) + \Delta(X_i)A_i)$, where Φ is the standard normal cumulative distribution function. Assuming the same priors for the parameters in θ as those for the continuous outcome case, the posterior is

$$p(\theta|X, A, Y) \propto p(Y|X, A, \theta)p(\theta) \propto \prod_{i=1}^n \Phi(f(X_i, A_i, \theta))^{Y_i} (1 - \Phi(f(X_i, A_i, \theta)))^{1-Y_i} p(\theta)$$

Sampling θ from this form is difficult. Thus, we consider the model augmented with a random variable Z .^{24;25} Specifically, we define independent latent variables Z_i , where each Z_i is normally distributed. Then the augmented probit model has the hierarchical structure as follows:

$$Y_i = \begin{cases} 1, & \text{if } Z_i > 0 \\ 0, & \text{if } Z_i \leq 0 \end{cases}$$

$$Z_i | \theta, X_i = \mu_i + \Delta_i A_i + \epsilon_i, \epsilon_i \sim N(0, 1)$$

$$\theta \sim p(\mu, \beta, l_\mu, \eta_\mu, \Delta, l_\Delta, \eta_\Delta)$$

Here, Y_i is deterministic conditional on the sign of Z_i .²⁶ Under the augmented model, $P(Y_i = 1 | X_i, A_i, \theta) = \Phi(f(X_i, A_i, \theta))$, so the two models give the same inference. We will employ the augmented model in sampling of the parameters of interest and the latent variables. The joint posterior of latent variables Z and model parameters θ given data X, A, Y is

$$p(Z, \theta | X, A, Y) \propto p(Z | X, A, Y, \theta) p(\theta) \\ \propto p(Z | \mu, \Delta, A, X, Y) p(\mu | \beta, l_\mu, \eta_\mu, X) p(\beta) p(l_\mu) p(\eta_\mu) p(\Delta | l_\Delta, \eta_\Delta) p(l_\Delta) p(\eta_\Delta)$$

where

$$p(\mu_i | \beta, l_\mu, \eta_\mu, X) = N(\mu | X\beta, \mathcal{K}_\mu) \\ p(\Delta | l_\Delta, \eta_\Delta, X) = N(\Delta | 0, \mathcal{K}_\Delta) \\ p(Z | \mu, \Delta, A, Y) = N(Z | \mu + \Delta A, 1) [I(Y = 1)I(Z > 0) + I(Y = 0)I(Z \leq 0)]$$

Note that θ is not dependent on Y given Z , so the conditional posterior of the model parameters θ is

$$p(\theta | Z, X) \propto p(\theta) N(Z | \mu + \Delta A, 1).$$

The conditional posterior of the latent variable Z_i is

$$Z_i | \theta, Y_i, X_i \sim \begin{cases} TN(\text{mean} = \mu_i + \Delta_i A_i, \text{sd} = 1, \text{lower} = 0, \text{upper} = \infty), & \text{if } Y_i = 1 \\ TN(\text{mean} = \mu_i + \Delta_i A_i, \text{sd} = 1, \text{lower} = -\infty, \text{upper} = 0), & \text{if } Y_i = 0 \end{cases}$$

Estimates of parameters are obtained by modifying the Metropolis within Gibbs algorithm such that Z_i takes the place of the continuous outcome and an additional step is used to sample Z_i from a truncated normal distribution.

Our interest is in the causal risk difference, $\Psi = P\{Y(1) = 1\} - P\{Y(0) = 1\}$. The posterior for Ψ can be obtained as follows. From the Gibbs sampler, we will have stored J draws of μ and Δ (after discarding burn-ins and thinning). At each iteration j , we obtain a draw of each potential outcome via computation. The probability of outcome under treatment, $p_1^{(j)} = P(Y(1) = 1)^{(j)}$, is

$$p_1^{(j)} = \frac{1}{n} \sum_{i=1}^n \Phi(\mu_i^{(j)} + \Delta_i^{(j)})$$

and the probability of the outcome in the absence of treatment is, $p_0^{(j)} = P(Y(0) = 1)^{(j)}$, is

$$p_0^{(j)} = \frac{1}{n} \sum_{i=1}^n \Phi(\mu_i^{(j)}).$$

Then the effect estimate at iteration j of the MCMC chain is $\Psi^{(j)} = p_1^{(j)} - p_0^{(j)}$. The estimate of the risk difference is the average difference in proportions over the J posterior samples: $\Psi = \frac{1}{J} \sum_j \Psi^{(j)}$.

3 Simulation Studies

Simulation studies were used to assess the performance of the GP model for scenarios with varying degrees of nonoverlap. In these, we considered both linear and nonlinear response surfaces with the latter including treatment heterogeneity and interactions between covariates. We compared our GP approach to the following methods:

BCF Bayesian causal forest with the prognostic and treatment components as functions of covariates and propensity scores, as proposed by Hahn et al. (2020).²⁰

BART-Stratified separate BART models are fit to treated and control subjects using covariates only and potential outcomes are estimated as the expected value of the function.²⁷

BART-Nethery untrimmed BART as implemented by Nethery et al. (2019) in which the treatment variable and propensity score are included as covariates, and potential outcomes are estimated with posterior predictive distributions.^{27;14}

BART+SPL the method proposed by Nethery et al. (2019) for nonoverlap using the recommended $a = .1, b = 10$ to define the region of overlap based on propensity scores.¹⁴

GLM generalized linear model regression of outcome on main effects of treatment indicator and covariates with identity link for continuous outcomes and probit link for binary outcomes.

For the Bayesian methods, MCMC specifications include 10,000 burn-ins and 5000 iterations after burn-ins, in which every 5th is kept, yielding 1000 posterior draws of the average treatment effect.

We use 1000 replications for the simulations. For each simulated data set, we obtain 1000 posterior estimates (after discarding burn ins and thinning) of treatment effect by averaging over all subjects. Specifically, for each replication k , we have 1000 posterior draws of the treatment component (average over individual causal effects at each iteration). Denote the estimate of the treatment effect, the mean over the posterior draws, by Ψ_k . The standard deviation SD_k and 95% credible intervals CI_k are obtained from these 1000 posterior draws. Over the 1000 replications we compute several quantities to measure performance:

$$ATE = \frac{1}{1000} \sum_{k=1}^{1000} \Psi_k$$

$$\overline{SD} = \frac{1}{1000} \sum_{k=1}^{1000} SD_k$$

$$Coverage = \frac{1}{1000} \sum_{k=1}^{1000} I(ATE_{true} \in CI_k)$$

$$\% \text{ Bias} = \frac{1}{1000} \sum_{k=1}^{1000} \left| \frac{\Psi_k - ATE_{true}}{ATE_{true}} \right| \cdot 100$$

$$SE = \sqrt{\frac{1}{1000 - 1} \sum_{k=1}^{1000} (\Psi_k - ATE)^2}$$

These simulations were conducted in R (R Core Team, 2020).²⁸

3.1 Continuous Outcome

For the setting with a continuous outcome, we generate treatment indicator A , two continuous covariates, and one binary covariate for $n = 500$ subjects. Our data generating model is specified as follows. First, treatment status is simulated as $A \sim \text{Bernoulli}(.5)$, and covariates are simulated based on treatment received. If $A = 1$, the covariates are generated as $X_1 \sim N(\mu_1, 1), X_2 \sim N(\mu_2, 1), X_3 \sim \text{Bernoulli}(p)$; if $A = 0$, $X_1 \sim N(0, 1), X_2 \sim N(2, 1), X_3 \sim \text{Bernoulli}(.4)$. We consider two different outcome models.

1. $Y_1 \sim N(1 - 2X_1 + X_2 - 1.2X_3 + 2A, 1)$
2. $Y_2 \sim N(-3 - 2.5X_1 + 2X_1^2A + \exp(1.4 - X_2A) + X_2X_3 - 1.2X_3 - 2X_3A + 2A, 1)$

Different combinations of μ_1 , μ_2 , and p are chosen to control the amount of covariate nonoverlap in the sample. We consider settings with some nonoverlap ($\mu_1 = 1, \mu_2 = 2, p = .5$) and substantial nonoverlap ($\mu_1 = 1, \mu_2 = 3, p = .6$). In the first model, the outcome is linearly related to covariates and treatment. In this case, for any combination of covariates, the treatment effect is the same—that is, treatment effect is homogeneous. We expect all methods to have decent performance since there are no interactions between covariates and treatment in the outcome model. Data generating model 2 incorporates nonlinearity and treatment heterogeneity. For instance, as X_1 values increase, the outcome Y for treated subjects tends to increase while Y values for control subjects tends to decrease. This leads to treatment effects that are larger in magnitude at larger X_1 values. Further, there is nonoverlap for these X_1 values since only treated subjects are observed in this region. The combination of treatment heterogeneity and nonoverlap makes it difficult to assess the treatment effect; parametric models would find it especially challenging to capture the true relationships.

We also consider the set of simulation scenarios in Nethery et al. (2019) since our primary comparative method is BART+SPL.¹⁴ We use scenarios for which BART+SPL had the best performance; this method underperforms when propensity scores are misspecified. For $n = 500$ subjects, half are assigned treatment $A = 1$ and half are assigned to $A = 0$. Here, c controls the degree of overlap. The values of c that are considered are 0, 0.35, 0.7, where larger values correspond to greater extents of nonoverlap. Covariates are generated based on treatment assignment. For treated subjects ($A = 1$), the covariates are generated with $X_1 \sim \text{Bernoulli}(.5)$, $X_2 \sim N(2 + c, (1.25 + .1c)^2)$. For control subjects ($A = 0$), $X_1 \sim \text{Bernoulli}(.4)$, $X_2 \sim N(1, 1)$. The true propensity score is calculated based on density functions as follows:

$$\text{True PS} = \frac{N(X_2; \mu = 2 + c, \sigma = 1.25 + .1c) \cdot \text{Ber}(X_1; p = .5)}{N(X_2; \mu = 2 + c, \sigma = 1.25 + .1c) \cdot \text{Ber}(X_1; p = .5) + N(X_2; \mu = 1, \sigma = 1) \cdot \text{Ber}(X_1; p = .4)}$$

The true potential outcomes under control and under treatment for all subjects are generated:

$$Y(0) = -1.5X_2,$$

$$Y(1) = \frac{-3}{1 + \exp(-10(X_2 - 1))} + .25X_1 - X_1X_2.$$

Then the true treatment effect for each person is $Y_i(1) - Y_i(0)$, so that there is a “true” ATE value for each simulated data set (say $ATE_{true,k}$ for the k th replication).

$$ATE_{true,k} = \frac{1}{N} \sum_{i=1}^N Y_i(1) - Y_i(0)$$

The observed outcome is taken to be $Y_i = A_iY_i(1) + (1 - A_i)Y_i(0)$.

Because there is a true ATE value for each replication indexed by k , for $k = 1, \dots, 1000$, we compute mean absolute bias instead of an overall ATE estimate.

$$\text{Abs Bias} = \frac{1}{1000} \sum_{k=1}^{1000} |\Psi_k - ATE_{true,k}|$$

The percent bias and coverage metrics are modified accordingly to accommodate different true values

across the replications.

$$\% \text{ Bias} = \frac{1}{1000} \sum_{k=1}^{1000} \left| \frac{\Psi_k - ATE_{true,k}}{ATE_{true,k}} \right| \cdot 100$$

$$\text{Coverage} = \frac{1}{1000} \sum_{k=1}^{1000} I(ATE_{true,k} \in CI_k).$$

3.1.1 Results

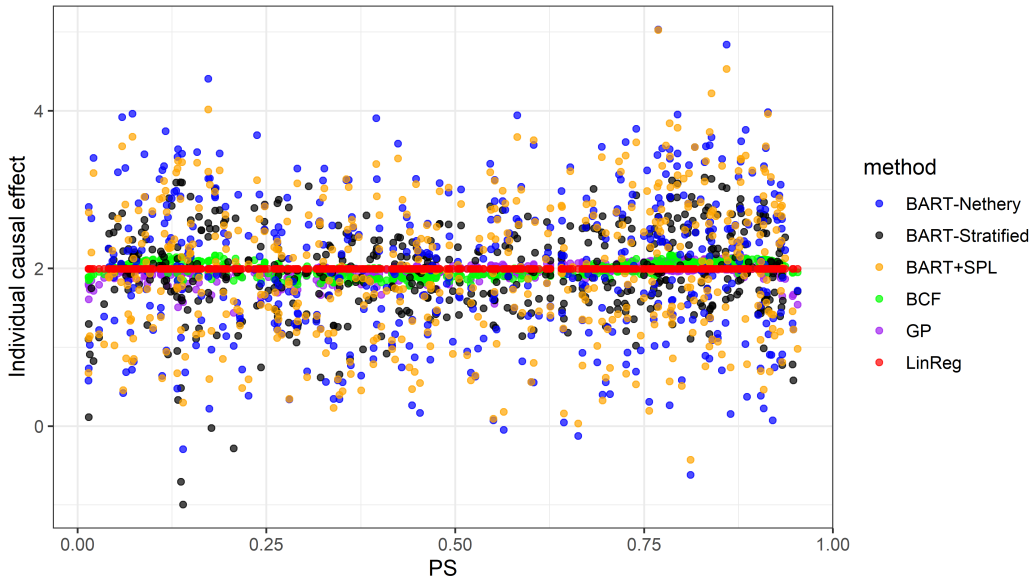
Simulation results for the nonoverlap scenarios in which the continuous outcomes are generated with a linear response surface are presented in Table 1. All methods provide estimates with low bias except BART-Stratified in the setting with some nonoverlap. We observe differences in the variability of the estimates. In particular, in the setting with some nonoverlap, the GP model’s estimate of variability is closest to that obtained from linear regression (the gold standard in this case). As the extent of nonoverlap increases, the variability obtained from the GP model increases to account for the greater uncertainty in those regions. On the other hand, the BART+SPL method results in coverage very close to 1 (indicating overcoverage).

Table 1: Effect estimates for nonoverlap scenarios involving a linear response surface across methods. The true ATE is 2 for both degrees of nonoverlap.

	Method	ATE	% Bias	\overline{SD}	SE	Coverage
Some nonoverlap	GP	1.968	4.167	.102	.099	.948
	BCF	2.002	4.108	.112	.104	.961
	BART-Stratified	1.904	5.991	.111	.113	.855
	BART-Nethery	2.011	4.225	.115	.106	.968
	BART+SPL (BART PS)	2.014	4.652	.156	.118	.980
	Linear model	1.998	3.906	.101	.098	.945
Substantial nonoverlap	GP	1.970	4.509	.115	.110	.947
	BCF	1.971	4.826	.130	.118	.962
	BART-Stratified	1.946	5.653	.136	.133	.927
	BART-Nethery	1.985	4.910	.137	.122	.965
	BART+SPL (BART PS)	1.976	6.665	.288	.175	.997
	Linear model	1.999	4.307	.112	.108	.955

To explore performance further, we next assess estimates of *individual* causal effects for each method using a simulated data set under each nonoverlap scenario. For the linear response surface under substantial nonoverlap, we plot estimates of posterior mean and posterior standard deviation of individual causal effects across the iterations for each subject (Figure 1). The analogous figure for the moderate nonoverlap setting is included as Supplementary Figure S1. The GP model provides estimates of individual causal effects that are close to 2 (the truth) indicating high precision, while those provided by BART-Nethery and BART+SPL are highly variable. Although the average treatment effect given by BART+SPL is close to the true value, the estimates of individual treatment effects range from -0.36 to 4.98.

a) Estimates of posterior mean individual causal effects (Substantial nonoverlap, Y_1)



b) Estimates of posterior SD individual causal effects (Substantial nonoverlap, Y_1)

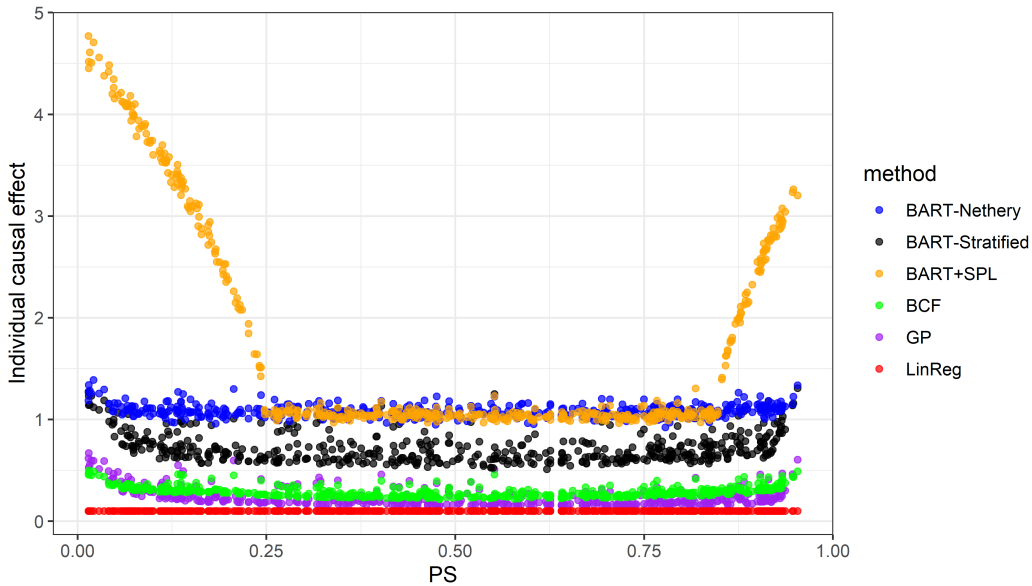


Figure 1: Individual causal effect exploration when outcome is generated with Y_1 for the substantial nonoverlap case.

The GP model tends to provide the lowest posterior standard deviations in regions of overlap. These estimates are only slightly greater than estimates of variability from linear regression, which would be correctly specified for this scenario. Because BART-Stratified and BART+SPL both model the treatment and control groups separately, baseline variability in estimates of treatment effect is higher. Notably, the Bayesian approaches show increases in variability in areas of increasing non-overlap, indicating that they are capturing the greater uncertainty in those regions. The GP model's estimates of individual-level standard deviations are greater than those of BCF in the nonoverlap areas; the continuous nature of the GP model means that uncertainty increases with covariate distance. However, the increase in the SD values when using BART+SPL is so steep that estimates for individuals

in the nonoverlap areas may hold little value.

Simulation results for data simulated using the second data generating model are given in Appendix B. For both degrees of nonoverlap, the GP model provided estimates with the smallest bias among the comparator methods. For this complex data scenario, linear regression has the worst performance as expected. The other nonparametric models, BCF, the two BART models, and BART+SPL all underestimate the average treatment effect with BART+SPL being the most biased. Note that the variability in the estimates of average treatment effect from the GP model again increase as the amount of nonoverlap increases as shown by \overline{SD} values. Thus, although there was bias from all the methods, the GP performed the best in terms of bias, efficiency, and coverage among the approaches considered.

Table 2 presents the simulation results using the scenarios from Nethery et al. (2019). For each degree of nonoverlap, the GP model results in the smallest bias—even under the settings where BART+SPL was previously shown to perform best.¹⁴ The GP model has coverage that is nearly the same as that of BART+SPL but has variability estimates that are smaller. The high coverage for the GP model indicates that it both accurately estimates the truth and translates the uncertainty from nonoverlap regions into higher variability. The greater than nominal coverage from the GP model for these scenarios may be due to the absence of an error term when outcomes were generated. In this scenario, estimates provided by the GP model had smaller bias than estimates from BCF. The increase in the variability estimates as the amount of nonoverlap grows is larger for the GP model than for the BART-only models (BCF, BART-Stratified, and BART-Nethery), better reflecting the extent of nonoverlap. Given the nonlinearity and interactions specified in the outcome model, the parametric linear regression has the worst performance as expected.

Table 2: Performance of the methods for nonoverlap scenarios from Nethery et al. (2019) that employ true propensity scores.

Setting	Method	Abs Bias	% Bias	\overline{SD}	SE	Coverage
c=0	GP	.007	2.758	.024	.051	1.000
	BCF	.034	13.511	.012	.057	.369
	BART-Stratified	.039	15.694	.014	.056	.378
	BART-Nethery	.028	11.137	.050	.056	.990
	BART+SPL	.014	5.500	.063	.054	1.000
	Linear model	.073	29.530	.082	.073	.941
c=.35	GP	.012	7.397	.030	.057	.998
	BCF	.057	35.406	.016	.067	.257
	BART-Stratified	.075	45.878	.020	.067	.204
	BART-Nethery	.050	30.922	.054	.068	.905
	BART+SPL	.022	13.212	.073	.060	1.000
	Linear model	.175	110.894	.093	.086	.546
c=.70	GP	.022	90.353	.041	.066	.995
	BCF	.091	342.029	.020	.081	.189
	BART-Stratified	.130	472.294	.026	.083	.123
	BART-Nethery	.082	314.237	.058	.085	.705
	BART+SPL	.034	102.883	.087	.070	.998
	Linear model	.316	1128.419	.106	.102	.137

In Figure 2, we display individual causal effects when there is moderate overlap (c=.35). The plots for c=0 and c=.70 are similar and are included as Supplementary Figures S2 and S3, respectively. In this scenario, it is clear that the BART-only methods tend to give constant estimates in regions of

nonoverlap (due to splitting on tails of covariate distributions) while the GP model and the BART+SPL model are able to capture the trends since their estimates of individual-level effects are closer to the true values. Thus, the BART-only methods underestimate the treatment effect in these areas. BART+SPL deems those with propensity scores larger than .75 to be in the region of nonoverlap, so that the posterior standard deviations increase substantially for these subjects. The increase in individual level posterior standard deviations for the GP model is more gradual. Further, the few treatment subjects relative to the number of control subjects with PS near 0 is reflected in the larger variability as estimated by the GP model for these regions. BART+SPL does not take this into account for the specified a and b values.

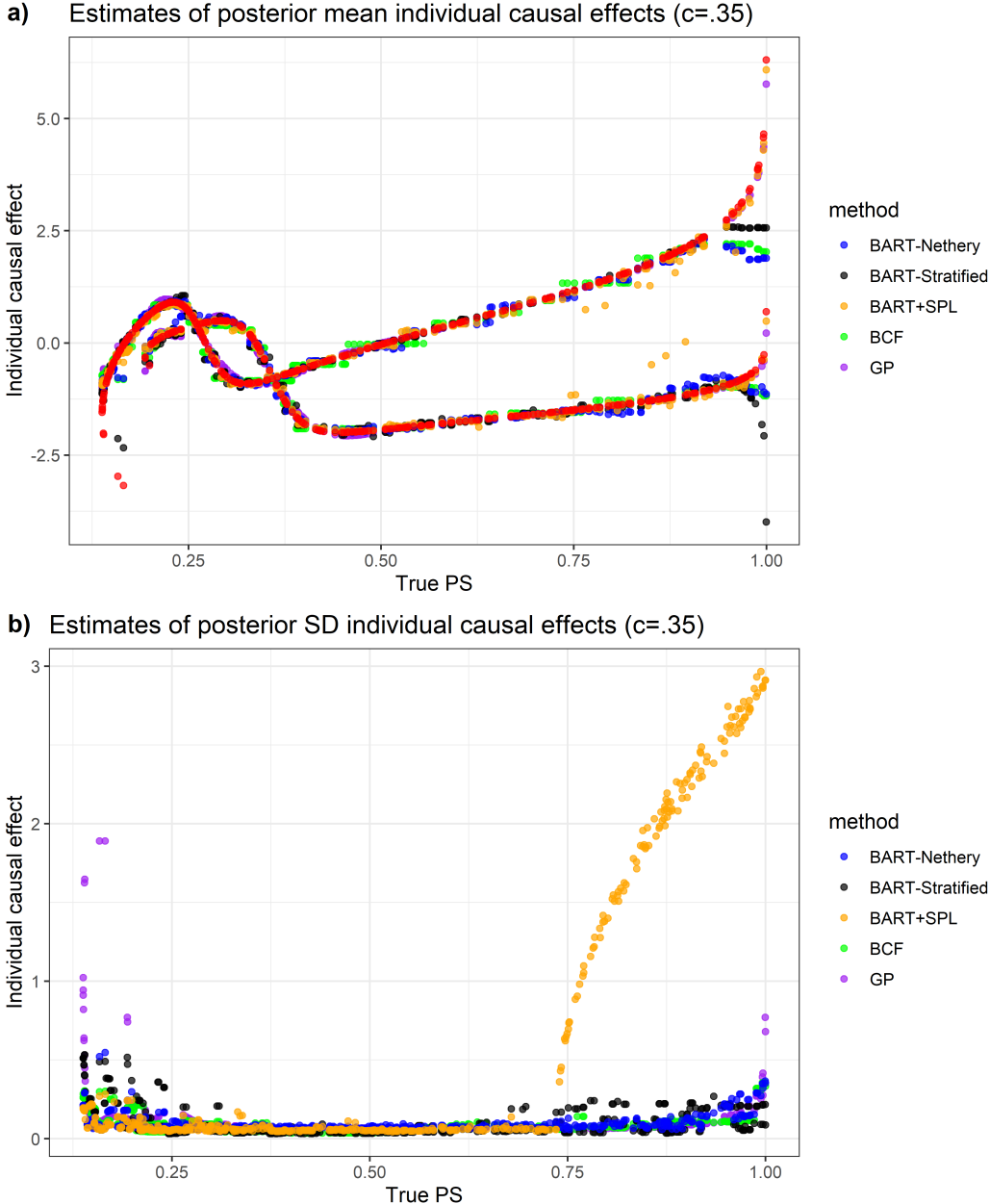


Figure 2: Individual-level posterior mean and standard deviation estimates from the methods considered. Red points denote the true individual causal effect based on the data generating model.

3.2 Binary Outcomes

In simulation studies for binary outcomes, the treatment indicator A and covariates X_1, X_2 , and X_3 are generated identically to the continuous case. We again consider two levels of nonoverlap and two outcome generating distributions. Outcomes are drawn from the Bernoulli distribution with proportion parameter that depends on covariate values and treatment received.

- $Y_{1B} \sim \text{Bernoulli}(\Phi(-1 - 2X_1 + X_2 - 1.2X_3 + 2A))$
- $Y_{2B} \sim \text{Bernoulli}(\Phi(-3 - 2.5X_1 + 2X_1^2A + \exp(1.4 - X_2A) + 1X_2X_3 - 1.2X_3 - 2X_3A + A))$

Detailed results of these simulations are provided in Appendix C. In brief, the GP model gives lower or similar bias and higher efficiency compared to the other methods and maintains its coverage when nonlinear and interaction terms are added to the outcome models.

4 Application to Study of Right Heart Catheterization

We applied our GP approach to data on critically ill patients in the Study to Understand Prognoses and Preferences for Outcomes and Risks of Treatments (SUPPORT). Details on the study population and data collection have been previously described in Connors et al. (1996).²⁹ We note that the purpose of this data example is to demonstrate our method and not to make clinical claims. These data are publicly available which will allow readers to readily replicate our results. In our analysis, we assess the effects of right heart catheterization (RHC) in the first 24 hours upon entry into study on survival for female subjects. The binary outcome of interest in this study is defined as

$$Y_i = \begin{cases} 1, & \text{if subject } i \text{ died within 180 days} \\ 0, & \text{otherwise} \end{cases}$$

The confounding variables of interest include age, race, years of education, income, medical insurance, primary disease category, Activities of Daily Living score, Duke Activity Status Index, do-not-resuscitate status, cancer status, SUPPORT model estimate of the probability of surviving 2 months, APACHE III score, coma score based on Glasgow on day 1, physiological measurements, and categories of comorbid illness. Of the 617 female subjects of interest, 137 received an RHC while 480 did not. In the treatment group, 62 died within 180 days, compared with 219 in the control group. Characteristics of the sample for analysis are provided in Supplementary Table 1. We see that the RHC group tends to be younger on average, have higher income, are less likely to sign a do-not-resuscitate form, and have lower respiratory rates and lower PaCO2 on Day 1. Further, the proportions of people with pulmonary disease were significantly different between the RHC and non-RHC groups. Propensity scores were estimated using a BART probit model with treatment status as the response and all confounding variables as predictors. Figure 3 demonstrates nonoverlap in the tails.

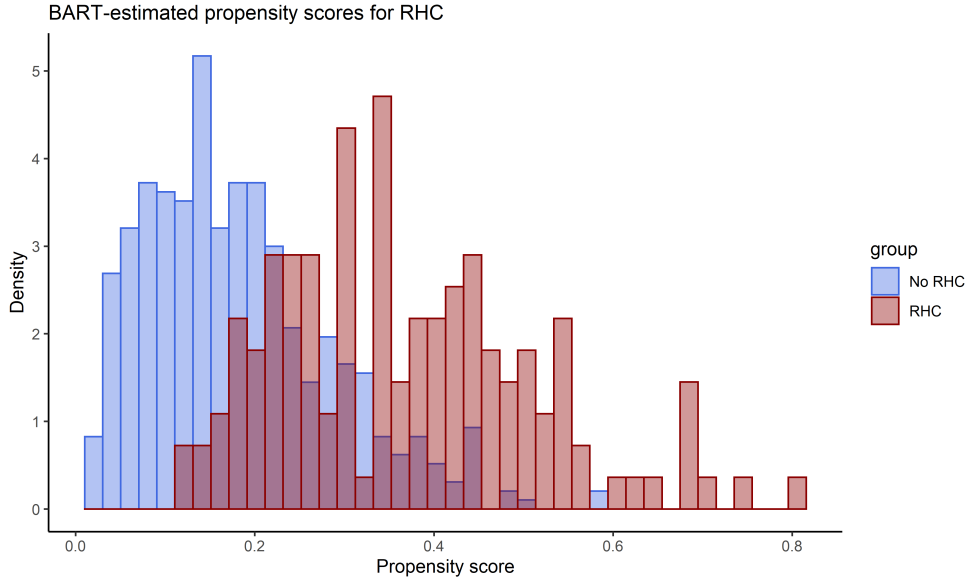


Figure 3: Histograms of estimated propensity scores for patients who received an RHC and those that did not.

To fit the Gaussian process model, we employed four chains with different initial values to estimate the parameters of interest. Specifically, each chain involved 10,000 burn-ins and 20,000 iterations after burn-ins, from which every 80th was kept in order to minimize autocorrelation. Combining these iterations, we obtained 1000 posterior draws for the parameters. We calculated a risk difference defined as the mean difference in probabilities of dying within 180 days from the start of study entry had the RHC been given versus had the RHC not been given, respectively. The risk difference estimate was 0.024 with 95% credible interval [-0.031, 0.098]. These estimates indicate that the 180-day survival of subjects who received the RHC did not differ significantly from that of patients who did not get RHC. Point estimates obtained from the comparator methods were found to be similar as shown in Table 3. In addition to having larger variability estimates for individuals in areas with less overlap, the GP model had the greatest efficiency in estimating the ATE compared to the other methods. BART+SPL resulted in the widest credible interval, which may be attributed to the method’s variance inflation factor for subjects in the nonoverlap region.

Table 3: Estimated average treatment effect of receiving the RHC.

	ATE	SE	95% CI
GP	.024	.033	[-.031, .098]
BCF	.033	.044	[-.047, .126]
BART-Stratified	.035	.049	[-.059, .124]
BART-Nethery	.031	.042	[-.049, .114]
BART+SPL	.030	.077	[-.111, .177]

5 Conclusion

In this paper, we develop a model that employs Gaussian process priors to address practical violations of the positivity assumption when estimating causal effects from observational data. Unlike matching or trimming approaches, our method allows inference about the original target population. Further,

unlike previous extrapolation methods, our approach does not require specifying arbitrary cut-offs in order to define nonoverlap regions. Importantly, our Gaussian process approach better reflects the greater uncertainty around estimated causal effects that is expected in areas of less covariate overlap.

For complex outcome models containing nonlinearities and interactions, the GP model provided average treatment effect estimates with good performance. This result may be attributed to the non-parametric nature of the GP model and the centering of the GP prior of the prognostic component on a linear model. By pulling the prior in the direction of the data, more accurate estimates were obtained in data sparse areas. Further, the form of our model places a direct prior on the treatment effect, which may be beneficial for incorporating prior knowledge of the treatment effect and for subsequent interpretation—the form of the posterior for treatment effects is known. The GP model also provided more accurate and precise estimates of individual causal effects, which were most likely due to its accommodation of each subject’s actual covariate values. For instance, for subjects in nonoverlap regions, we observed the GP model to be superior to the BART models in providing individual-level estimates that are close to the truth.

One current limitation to our approach is the potential lack of scalability to very large studies due to computational challenges. The computational complexity is $\mathcal{O}(n^3)$ due to inversion of matrices that have dimensions equal to the sample size. Further, the long run time may be due to the number of parameters being sampled in our Markov Chain Monte Carlo; our algorithm estimates hyperparameters rather than fixing them at constant values. Our efforts to reduce computation time include employing Cholesky decomposition and sampling parameters from their conditional distribution when possible. Future work could focus on optimizing computational efficiency. Moreover, here we have focused on continuous and binary outcomes. We are currently considering extensions of the GP approach to other outcomes that are common in clinical studies such as censored survival outcomes and longitudinal outcomes. In the longitudinal setting, addressing positivity violations may pose particular challenges due to time-dependent confounding.

6 Appendix

A Conditional distributions for μ , β , and Δ

For the choice of prior for the hyperparameter β in the GP prior for μ is

$p(\beta) \propto \det(\sigma_\beta^2 I_P)^{-1/2} \exp\left\{-\frac{1}{2}\beta^T(\sigma_\beta^2 I_P)^{-1}\beta\right\}$, the conditional posterior distribution for β is

$$\begin{aligned}
p(\beta|\mu, y) &\propto p(y|\mu, \beta)p(\mu|\beta)p(\beta) \\
&\propto \exp\left[-\frac{1}{2}\{y - (\mu + \Delta A)\}^T (\sigma^2 I)^{-1} \{y - (\mu + \Delta A)\}\right] \exp\left\{-\frac{1}{2}(\mu - X\beta)^T K_\mu^{-1}(\mu - X\beta)\right\} \exp\left\{-\frac{1}{2}\beta^T(\sigma_\beta^2 I_P)^{-1}\beta\right\} \\
&\propto \exp\left[-\frac{1}{2}\left\{\mu^T K_\mu^{-1}\mu - 2\mu^T K_\mu^{-1}X\beta + \beta^T X^T K_\mu^{-1}X\beta + \beta^T(\sigma_\beta^2 I_P)^{-1}\beta\right\}\right] \\
&\propto \exp\left(-\frac{1}{2}\left[\beta^T \left\{X^T K_\mu^{-1}X + (\sigma_\beta^2 I_P)^{-1}\right\}\beta - 2\beta^T X^T K_\mu^{-1}\mu\right]\right) \\
&\propto \exp\left[-\frac{1}{2}\left(\beta^T \left\{X^T K_\mu^{-1}X + (\sigma_\beta^2 I_P)^{-1}\right\}\beta - 2\beta^T \left\{X^T K_\mu^{-1}X + (\sigma_\beta^2 I_P)^{-1}\right\}\left\{X^T K_\mu^{-1}X + (\sigma_\beta^2 I_P)^{-1}\right\}^{-1} X^T K_\mu^{-1}\mu\right.\right. \\
&\quad \left.\left.+ \left[\left\{X^T K_\mu^{-1}X + (\sigma_\beta^2 I_P)^{-1}\right\}^{-1} X^T K_\mu^{-1}\mu\right]^T \left\{X^T K_\mu^{-1}X + (\sigma_\beta^2 I_P)^{-1}\right\} \left[\left\{X^T K_\mu^{-1}X + (\sigma_\beta^2 I_P)^{-1}\right\}^{-1} X^T K_\mu^{-1}\mu\right]\right)\right] \\
&\propto \exp\left(-\frac{1}{2}\left[\beta - \left\{X^T K_\mu^{-1}X + (\sigma_\beta^2 I_P)^{-1}\right\}^{-1} X^T K_\mu^{-1}\mu\right]^T \left\{X^T K_\mu^{-1}X + (\sigma_\beta^2 I_P)^{-1}\right\} \left[\beta - \left\{X^T K_\mu^{-1}X + (\sigma_\beta^2 I_P)^{-1}\right\}^{-1} X^T K_\mu^{-1}\mu\right]\right)
\end{aligned}$$

Thus, $\beta|\mu, y \sim MVN \left(\left[X^T K_\mu^{-1} X + (\sigma_\beta^2 I_P)^{-1} \right]^{-1} X^T K_\mu^{-1} \mu, \left[X^T K_\mu^{-1} X + (\sigma_\beta^2 I_P)^{-1} \right]^{-1} \right)$.

The prior for μ is $p(\mu) \propto \det(K_\mu)^{-\frac{1}{2}} \exp \left[-\frac{1}{2} (\mu - X\beta)^T K_\mu^{-1} (\mu - X\beta) \right]$.

The prior for Δ is $p(\Delta) \propto \det(K_\Delta)^{-\frac{1}{2}} \exp \left[-\frac{1}{2} \Delta^T K_\Delta^{-1} \Delta \right]$.

Assuming prior independence of μ and Δ , $p(\mu, \Delta) = p(\mu)p(\Delta)$, the joint posterior is

$$\begin{aligned} p(\mu, \Delta|y) &\propto p(y|\mu, \Delta)p(\mu, \Delta) \\ &\propto p(y|\mu, \Delta)p(\mu)p(\Delta) \end{aligned}$$

The posterior distributions for μ and Δ are obtained as follows.

The posterior for $\mu|\Delta, y$ is given by

$$\begin{aligned} p(\mu|\Delta, y) &\propto p(y|\mu, \Delta)p(\mu) \\ &\propto \det(\sigma^2 I)^{-\frac{1}{2}} \exp \left[-\frac{1}{2} \{y - (\mu + \Delta A)\}^T (\sigma^2 I)^{-1} \{y - (\mu + \Delta A)\} \right] \det(K_\mu)^{-\frac{1}{2}} \exp \left[-\frac{1}{2} (\mu - X\beta)^T K_\mu^{-1} (\mu - X\beta) \right] \\ &\propto \exp \left(-\frac{1}{2} \left[\{y - (\mu + \Delta A)\}^T (\sigma^2 I)^{-1} \{y - (\mu + \Delta A)\} + (\mu - X\beta)^T K_\mu^{-1} (\mu - X\beta) \right] \right) \\ &\propto \exp \left[-\frac{1}{2} \left\{ y^T (\sigma^2 I)^{-1} y - 2y^T (\sigma^2 I)^{-1} (\mu + \Delta A) + (\mu + \Delta A)^T (\sigma^2 I)^{-1} (\mu + \Delta A) + \mu^T K_\mu^{-1} \mu - 2\mu^T K_\mu^{-1} X\beta + (X\beta)^T K_\mu^{-1} X\beta \right\} \right] \\ &\propto \exp \left[-\frac{1}{2} \left\{ -2\mu^T (\sigma^2 I)^{-1} y + \mu^T (\sigma^2 I)^{-1} \mu + 2\mu^T (\sigma^2 I)^{-1} \Delta A + \mu^T K_\mu^{-1} \mu - 2\mu^T K_\mu^{-1} X\beta \right\} \right] \\ &\propto \exp \left(-\frac{1}{2} \left[\mu^T \left\{ K_\mu^{-1} + (\sigma^2 I)^{-1} \right\} \mu - 2\mu^T \left\{ (\sigma^2 I)^{-1} y - (\sigma^2 I)^{-1} \Delta A + K_\mu^{-1} X\beta \right\} \right] \right) \\ &\propto \exp \left[-\frac{1}{2} \left(\mu^T \left\{ K_\mu^{-1} + (\sigma^2 I)^{-1} \right\} \mu - 2\mu^T \left\{ K_\mu^{-1} + (\sigma^2 I)^{-1} \right\} \left\{ K_\mu^{-1} + (\sigma^2 I)^{-1} \right\}^{-1} \left\{ (\sigma^2 I)^{-1} (y - \Delta A) + K_\mu^{-1} X\beta \right\} \right. \right. \\ &\quad \left. \left. + \left[\left\{ K_\mu^{-1} + (\sigma^2 I)^{-1} \right\}^{-1} \left\{ (\sigma^2 I)^{-1} (y - \Delta A) + K_\mu^{-1} X\beta \right\} \right]^T \left\{ K_\mu^{-1} + (\sigma^2 I)^{-1} \right\} \right. \right. \\ &\quad \left. \left. \times \left\{ K_\mu^{-1} + (\sigma^2 I)^{-1} \right\}^{-1} \left\{ (\sigma^2 I)^{-1} (y - \Delta A) + K_\mu^{-1} X\beta \right\} \right] \right) \\ &\propto \exp \left(-\frac{1}{2} \left[\mu - \left\{ K_\mu^{-1} + (\sigma^2 I)^{-1} \right\}^{-1} \left\{ (\sigma^2 I)^{-1} (y - \Delta A) + K_\mu^{-1} X\beta \right\} \right]^T \left\{ K_\mu^{-1} + (\sigma^2 I)^{-1} \right\} \right. \\ &\quad \left. \left[\mu - \left\{ K_\mu^{-1} + (\sigma^2 I)^{-1} \right\}^{-1} \left\{ (\sigma^2 I)^{-1} (y - \Delta A) + K_\mu^{-1} X\beta \right\} \right] \right) \end{aligned}$$

Thus, $\mu|\Delta, y \sim MVN \left(\left[K_\mu^{-1} + (\sigma^2 I)^{-1} \right]^{-1} \left[(\sigma^2 I)^{-1} (y - \Delta A) + K_\mu^{-1} X\beta \right], \left[K_\mu^{-1} + (\sigma^2 I)^{-1} \right]^{-1} \right)$.

The posterior for $\Delta|\mu, y$ is given by

$$\begin{aligned}
p(\Delta|\mu, y) &\propto p(y|\mu, \Delta)p(\Delta) \\
&\propto \det(\sigma^2 I)^{-\frac{1}{2}} \exp \left[\{y - (\mu + \Delta A)\}^T (\sigma^2 I)^{-1} \{y - (\mu + \Delta A)\} \right] \det(K_\Delta)^{-\frac{1}{2}} \exp \left(-\frac{1}{2} \Delta^T K_\Delta^{-1} \Delta \right) \\
&\propto \exp \left[-\frac{1}{2} \left\{ y^T (\sigma^2 I)^{-1} y - 2y^T (\sigma^2 I)^{-1} (\mu + \Delta A) + (\mu + \Delta A)^T (\sigma^2 I)^{-1} (\mu + \Delta A) + \Delta^T K_\Delta^{-1} \Delta \right\} \right] \\
&\propto \exp \left[-\frac{1}{2} \left\{ -2(\Delta A)^T (\sigma^2 I)^{-1} y + \mu^T (\sigma^2 I)^{-1} \mu + 2(\Delta A)^T (\sigma^2 I)^{-1} \mu + (\Delta A)^T (\sigma^2 I)^{-1} \Delta A + \Delta^T K_\Delta^{-1} \Delta \right\} \right] \\
&\propto \exp \left(-\frac{1}{2} \left[\Delta^T \left\{ A^T \odot (\sigma^2 I)^{-1} \odot A + K_\Delta^{-1} \right\} \Delta - 2\Delta^T \left\{ A^T \odot (\sigma^2 I)^{-1} (y - \mu) \right\} \right] \right) \\
&\propto \exp \left(-\frac{1}{2} \left[\Delta^T \left\{ K_\Delta^{-1} + A^T \odot (\sigma^2 I)^{-1} \odot A \right\} \Delta - 2\Delta^T \left\{ K_\Delta^{-1} + A^T \odot (\sigma^2 I)^{-1} \odot A \right\} \left\{ K_\Delta^{-1} + A^T \odot (\sigma^2 I)^{-1} \odot A \right\}^{-1} \right. \right. \\
&\quad \left. \left. \left\{ A^T \odot (\sigma^2 I)^{-1} (y - \mu) \right\} + (y - \mu)^T \left[\left\{ K_\Delta^{-1} + A^T \odot (\sigma^2 I)^{-1} \odot A \right\}^{-1} A^T \odot (\sigma^2 I)^{-1} \right]^T \right. \right. \\
&\quad \left. \left. \left\{ K_\Delta^{-1} + A^T \odot (\sigma^2 I)^{-1} \odot A \right\} \left\{ K_\Delta^{-1} + A^T \odot (\sigma^2 I)^{-1} \odot A \right\}^{-1} A^T \odot (\sigma^2 I)^{-1} (y - \mu) \right] \right) \\
&\propto \exp \left(-\frac{1}{2} \left[\Delta - \left\{ K_\Delta^{-1} + A^T \odot (\sigma^2 I)^{-1} \odot A \right\}^{-1} A^T \odot (\sigma^2 I)^{-1} (y - \mu) \right]^T \left\{ K_\Delta^{-1} + A^T \odot (\sigma^2 I)^{-1} \odot A \right\} \right. \\
&\quad \left. \left[\Delta - \left\{ K_\Delta^{-1} + A^T \odot (\sigma^2 I)^{-1} \odot A \right\}^{-1} A^T \odot (\sigma^2 I)^{-1} (y - \mu) \right] \right)
\end{aligned}$$

Thus, $\Delta|\mu, y \sim MVN \left(\left[K_\Delta^{-1} + A^T \odot (\sigma^2 I)^{-1} \odot A \right]^{-1} A^T \odot (\sigma^2 I)^{-1} (y - \mu), \left[K_\Delta^{-1} + A^T \odot (\sigma^2 I)^{-1} \odot A \right]^{-1} \right)$.

B Results for Continuous Outcome Scenario Involving Nonlinearity and Treatment Heterogeneity

Table 4: Effect estimates for nonoverlap scenarios involving a nonlinear response surface and treatment heterogeneity. The true ATE for the some nonoverlap and substantial nonoverlap settings are .950 and .564, respectively.

	Method	ATE	% Bias	SD	SE	Coverage
Some nonoverlap	GP	.849	20.530	.119	.225	.657
	BCF	.814	24.011	.140	.251	.658
	BART-Stratified	.758	26.188	.118	.237	.535
	BART-Nethery	.658	33.889	.205	.252	.667
	BART+SPL	.580	41.407	.254	.285	.689
	LinReg	-.049	105.120	.315	.279	.082
Substantial nonoverlap	GP	.429	40.201	.157	.251	.727
	BCF	.349	48.496	.168	.256	.663
	BART-Stratified	.334	47.961	.148	.247	.588
	BART-Nethery	.190	69.222	.218	.258	.589
	BART+SPL	.013	100.999	.386	.357	.707
	LinReg	-.562	199.632	.338	.319	.088

Figure 4 and 5 provide further information regarding individual causal effects estimated by each method. The GP model is able to capture the larger average treatment effects for subjects with estimated propensity scores near 0, which helps to pull up its estimates of the ATE. Furthermore,

for these subjects, estimates of posterior standard deviations obtained from the GP model are larger than those from both BART models. This suggests that the continuous nature of the GP model better allows larger distances to be translated into greater estimates of uncertainty as compared to the BART models. On the other hand, BART+SPL's variation inflation factor greatly overestimates the corresponding uncertainty, which results in inconsequential knowledge about the treatment effects for subjects in nonoverlap areas.

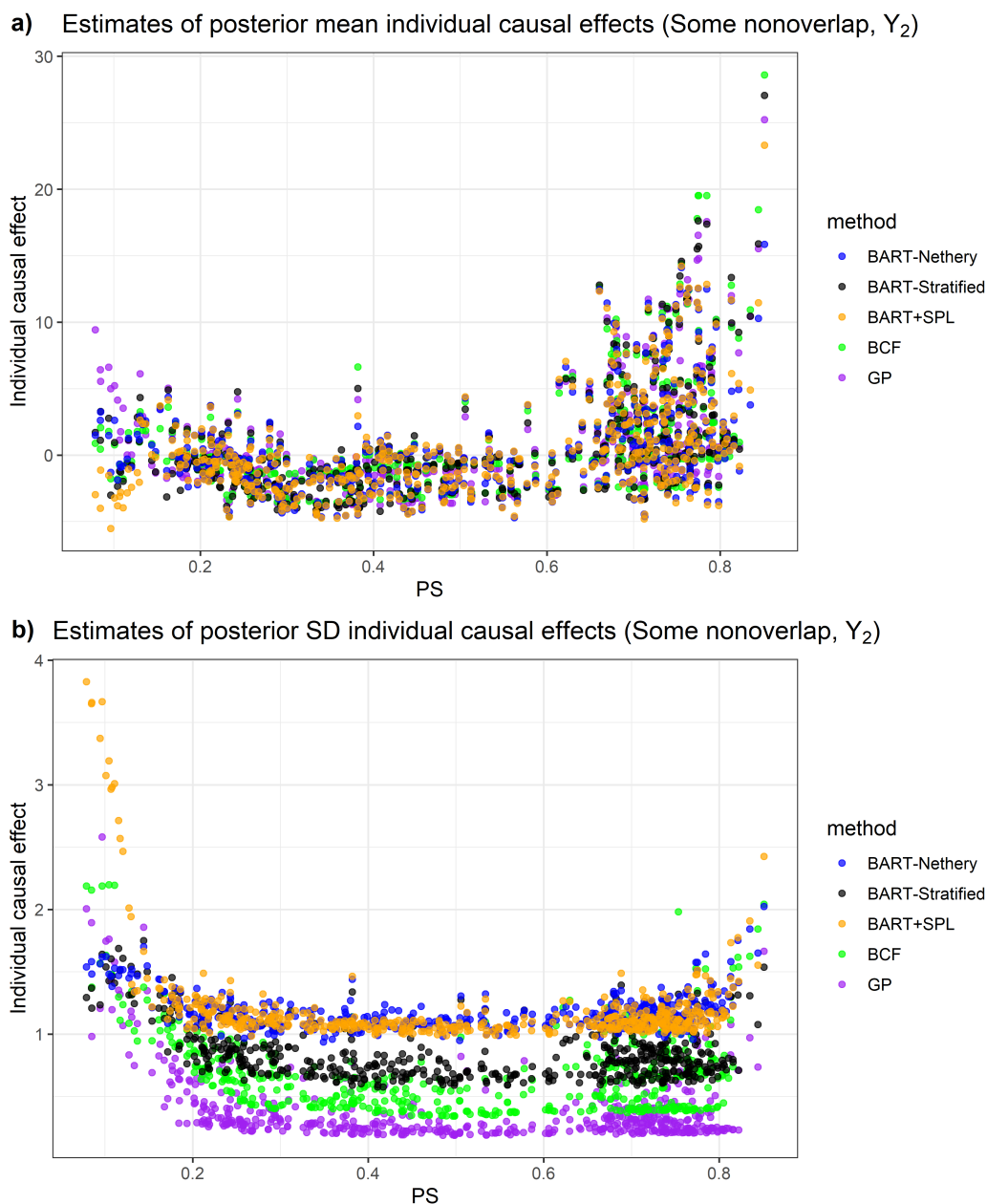
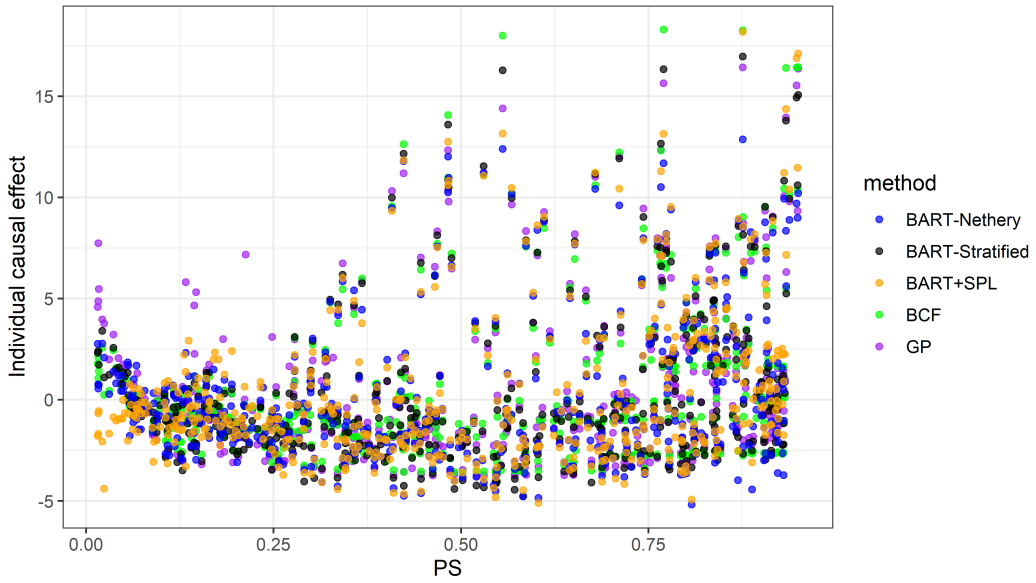


Figure 4: Individual causal effect exploration when the continuous outcome is generated with Y_2 for the some nonoverlap setting.

a) Estimates of posterior mean individual causal effects (Substantial nonoverlap, Y_2)



b) Estimates of posterior SD individual causal effects (Substantial nonoverlap, Y_2)

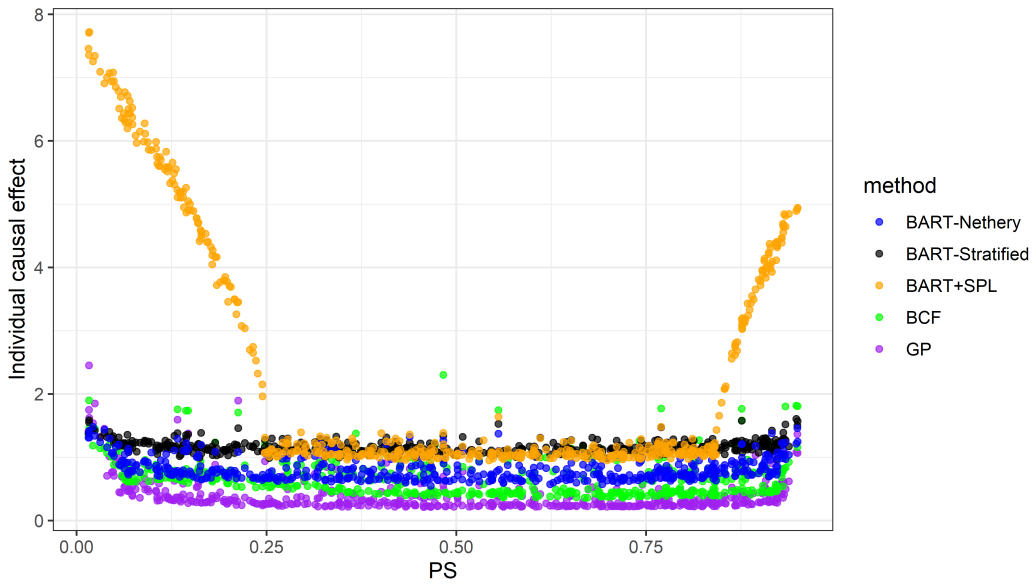


Figure 5: Individual causal effect exploration when the continuous outcome is generated with Y_2 for the substantial nonoverlap setting.

C Results for Binary Outcomes

Table 5: Effect estimates from each method for nonoverlap scenarios involving a outcome model (Y_{1B}) that is linear on the probit scale. The true ATE is .280 for the some nonoverlap setting and .283 for the substantial nonoverlap setting.

	Method	ATE	% Bias	\overline{SD}	SE	Coverage
Some nonoverlap	GP	.269	7.970	.024	.026	.902
	BCF	.300	10.103	.035	.028	.957
	BART-Stratified	.249	12.255	.030	.028	.833
	BART-Nethery	.270	7.812	.028	.026	.947
	BART+SPL	.276	9.166	.033	.033	.952
	Probit model	.279	7.351	.011	.026	.614
Substantial nonoverlap	GP	.274	9.485	.030	.032	.916
	BCF	.279	10.081	.041	.036	.976
	BART-Stratified	.267	10.551	.039	.034	.964
	BART-Nethery	.271	9.539	.036	.031	.970
	BART+SPL	.280	12.240	.054	.043	.984
	Probit model	.283	8.916	.011	.031	.517

Table 6: Effect estimates from each method for nonoverlap scenarios involving a outcome model (Y_{2B}) that is nonlinear and involves interactions on the probit scale. The true ATE is -.146 for the some nonoverlap setting and -.202 for the substantial nonoverlap setting.

	Method	ATE	% Bias	\overline{SD}	SE	Coverage
Some nonoverlap	GP	-.157	20.585	.029	.036	.863
	BCF	-.148	20.872	.031	.038	.882
	BART-Stratified	-.197	37.323	.037	.038	.697
	BART-Nethery	-.199	38.843	.044	.040	.790
	BART+SPL	-.213	48.674	.050	.051	.736
	Probit model	-.259	77.632	.001	.048	.001
Substantial nonoverlap	GP	-.221	17.752	.038	.042	.893
	BCF	-.212	18.575	.038	.047	.877
	BART-Stratified	-.254	27.761	.043	.043	.781
	BART-Nethery	-.268	33.627	.046	.045	.750
	BART+SPL	-.297	47.480	.066	.057	.729
	Probit model	-.332	64.115	.001	.052	0

References

- [1] Hernán MA, Robins JM. Estimating Causal Effects from Epidemiological Data. Journal of epidemiology and community health. 2006-07;60(7):578–586.
- [2] Westreich D, Cole SR. Invited Commentary: Positivity in Practice. American journal of epidemiology. 2010-03-15;171(6):674–7; discussion 678–681.
- [3] Imbens GW, Rubin DB. Assessing Overlap in Covariate Distributions. In: Causal Inference for

- Statistics, Social, and Biomedical Sciences: An Introduction. Cambridge University Press; 2015. p. 309–336.
- [4] D’Amour A, Ding P, Feller A, Lei L, Sekhon J. Overlap in Observational Studies with High-Dimensional Covariates. *Journal of Econometrics*. 2020.
 - [5] King G, Zeng L. The Dangers of Extreme Counterfactuals. *Political Analysis*. 2006;14(2):131–159.
 - [6] Petersen ML, Porter KE, Gruber S, Wang Y, van der Laan MJ. Diagnosing and Responding to Violations in the Positivity Assumption. *Statistical Methods in Medical Research*. 2012;21(1):31–54.
 - [7] Crump RK, Hotz VJ, Imbens GW, Mitnik OA. Dealing with Limited Overlap in Estimation of Average Treatment Effects. *Biometrika*. 2009;96(1):187–199.
 - [8] Rosenbaum PR. Optimal Matching of an Optimally Chosen Subset in Observational Studies. *Journal of Computational and Graphical Statistics*. 2012;21(1):57–71.
 - [9] Visconti G, Zubizarreta J. Handling Limited Overlap in Observational Studies with Cardinality Matching. *Observational Studies*. 2018;4:217–249.
 - [10] Hill J, Su YS. Assessing Lack of Common Support in Causal Inference Using Bayesian Nonparametrics: Implications for Evaluating the Effect of Breastfeeding on Children’s Cognitive Outcomes. *The Annals of Applied Statistics*. 2013-09;7(3):1386–1420.
 - [11] Ghosh D. Relaxed Covariate Overlap and Margin-Based Causal Effect Estimation. *Statistics in Medicine*. 2018;37(28):4252–4265.
 - [12] Li F, Morgan KL, Zaslavsky AM. Balancing Covariates via Propensity Score Weighting. *Journal of the American Statistical Association*. 2018;113(521):390–400.
 - [13] Li F, Thomas LE, Li F. Addressing Extreme Propensity Scores via the Overlap Weights. *American journal of epidemiology*. 2019;188(1):250–257.
 - [14] Nethery RC, Mealli F, Francesca D. Estimating Population Average Causal Effects in the Presence of Non-Overlap: The Effect of Natural Gas Compressor Station Exposure on Cancer Mortality. *The Annals of Applied Statistics*. 2019;13(2):1242–1267.
 - [15] Rasmussen CE, Williams CKI. *Gaussian Processes for Machine Learning*. The MIT Press. Massachusetts Institute of Technology; 2006.
 - [16] Neal RM. Regression and Classification Using Gaussian Process Priors. *Bayesian Statistics 6*. 1998.
 - [17] Rubin DB. Causal Inference Using Potential Outcomes. *Journal of the American Statistical Association*. 2005;100(469):322–331.
 - [18] Rosenbaum PR, Rubin DB. The Central Role of the Propensity Score in Observational Studies for Causal Effects. *Biometrika*. 1983;70(1):41–55.
 - [19] Rubin DB. The Design versus the Analysis of Observational Studies for Causal Effects: Parallels with the Design of Randomized Trials. *Statistics in Medicine*. 2007;26(1):20–36.

- [20] Hahn PR, Murray JS, Carvalho CM. Bayesian Regression Tree Models for Causal Inference: Regularization, Confounding, and Heterogeneous Effects (with Discussion). *Bayesian Anal.* 2020-09;15(3):965–1056.
- [21] Craiu RV, Rosenthal JS. Bayesian Computation Via Markov Chain Monte Carlo. *Annual Review of Statistics and Its Application.* 2014;1(1):179–201.
- [22] Gelfand AE. Gibbs Sampling. *Journal of the American Statistical Association.* 2000;95(452):1300–1304.
- [23] Casella G, George EI. Explaining the Gibbs Sampler. *The American Statistician.* 1992;46(3):167–174.
- [24] Meng XL, Van Dyk DA. Seeking Efficient Data Augmentation Schemes via Conditional and Marginal Augmentation. *Biometrika.* 1999;86(2):301–320.
- [25] Van Dyk DA, Meng XL. The Art of Data Augmentation. *Journal of Computational and Graphical Statistics.* 2001;10(1):1–50.
- [26] Albert JH, Chib S. Bayesian Analysis of Binary and Polychotomous Response Data. *Journal of the American Statistical Association.* 1993-06-01;88(422):669–679.
- [27] Chipman HA, George EI, McCulloch RE. BART: Bayesian Additive Regression Trees. *The Annals of Applied Statistics.* 2010;4(1):266–298.
- [28] R Core Team. *R: A Language and Environment for Statistical Computing.* Vienna, Austria; 2020.
- [29] Connors AFJ, Speroff T, Dawson NV, Thomas C, Harrell FEJ, Wagner D, et al. The Effectiveness of Right Heart Catheterization in the Initial Care of Critically Ill Patients. SUPPORT Investigators. *JAMA.* 1996;276(11):889–897.
- [30] Dehejia R, Wahba S. Propensity Score Matching Methods For Non-Experimental Causal Studies. *The Review of Economics and Statistics.* 2002;84:151–161.